

# *Comparison of two soft chemistry routes for the synthesis of mesoporous carbon/ $\beta$ -SiC nanocomposites*

**Xavier Deschanel, Damien Hérault, Guilhem Arrachart, Cyrielle Rey, Agnès Grandjean, Guillaume Toquer, Renaud Podor, Thomas Zemb, et al.**

**Journal of Materials Science**  
Full Set - Includes 'Journal of Materials Science Letters'

ISSN 0022-2461

J Mater Sci  
DOI 10.1007/s10853-013-7222-z



**Your article is protected by copyright and all rights are held exclusively by Springer Science +Business Media New York. This e-offprint is for personal use only and shall not be self-archived in electronic repositories. If you wish to self-archive your work, please use the accepted author's version for posting to your own website or your institution's repository. You may further deposit the accepted author's version on a funder's repository at a funder's request, provided it is not made publicly available until 12 months after publication.**

# Comparison of two soft chemistry routes for the synthesis of mesoporous carbon/ $\beta$ -SiC nanocomposites

Xavier Deschanel · Damien Hérault · Guilhem Arrachart · Cyrielle Rey ·  
Agnès Grandjean · Guillaume Toquer · Renaud Podor · Thomas Zemb ·  
Geneviève Cerveau · Robert Corriu

Received: 8 October 2012 / Accepted: 5 February 2013  
© Springer Science+Business Media New York 2013

**Abstract** We compare the influence of using either molecular or colloidal precursors on the synthesis of a ceramic material containing SiC and porous carbon. Remarkably, the temperature of synthesis for crystalline SiC is independent of the route chosen. The excess carbon in the initial mixture is the source of the excess porous carbon that binds to the crystalline domains of SiC in the final products. Interestingly, increasing the initial area of surface contact between carbon and silicon in the ceramic precursor results in different porosities in the ‘meso’ range. Simultaneous control of the size and the relative amounts of Si and C in the precursors allows control to be exerted over the nature and texture of the final powders. A simple and general mechanism is herein proposed to explain the evolution of the surface area as a function of the volume fraction of residual carbon in the synthesised ceramic.

## Introduction

Silicon carbide is a compound with excellent mechanical strength, thermal stability and good thermal conductivity properties. Because of these properties, SiC is used in advanced ceramics applications, such as electronics (diodes, semi-conductor devices), technical ceramics (cutting tools, abrasive, brake discs, heating elements) and catalysis (support at extreme process conditions), as well as in the nuclear industry (expansion layers for the nuclear fuel elements of high temperature reactors) [1–4]. The Acheson [5] process is generally used in industry for the production of silicon carbides. This process includes the carbothermal reduction of silica sand by petrol coke. The main drawback of this process is its high temperature reaction conditions (1800–2200 °C), which lead to coarse-grained powders with low surface areas (0.1–15 m<sup>2</sup>/g) [6].

One manner of lowering the temperature of this synthesis is to reduce the size of the initial products from the micrometric to the nanometric scale [7]. The ultimate reduction via increasing the initial area of contact is to use, even in the precursors, the Si–C already formed. Along this line, the strategy is to include C and Si in the same ‘precursor’ molecule. A recent review shows examples of size-dependent effects in nanomaterials [8]; for example, the melting temperature of 2.5 nm gold particles was reported to be approximately 930 K, a value much lower than that of bulk gold, 1336 K [9]. This discrepancy corresponds to the larger fraction of atoms located at the surface of the nanomaterials relative to the fraction of atoms at the surface of bulk gold.

Previous studies [10–16] suggest that the temperature of the carbothermal reduction of SiO<sub>2</sub> by carbon decreases when colloidal or nanometric precursors are involved in the reaction. Martin [13, 14] used nanosized precursors

**Electronic supplementary material** The online version of this article (doi:10.1007/s10853-013-7222-z) contains supplementary material, which is available to authorized users.

X. Deschanel (✉) · G. Arrachart · C. Rey · A. Grandjean ·  
G. Toquer · R. Podor · T. Zemb  
ICSM-UMR 5257, CEA/CNRS/UM2/ENSCM Marcoule,  
BP 17171, 30207 Bagnols-sur-Cèze, France  
e-mail: xavier.deschanel@cea.fr

D. Hérault  
Centrale Marseille, Aix Marseille Université, CNRS,  
iSm2 UMR 7313, 13397 Marseille, France

G. Cerveau · R. Corriu  
Institut Charles Gerhardt, UMR 5253,  
Université de Montpellier 2, 34095 Montpellier, France

(colloidal silica and sugar) to synthesise  $\beta$ -SiC at temperatures as low as 1300 °C. Kevorkijan [10] and Krstic [16] synthesised  $\beta$ -SiC powders by the carbothermic reduction of carbon black and colloidal silica at temperatures ranging from 1330 to 1800 °C. Lin [11] studied the effects of the starting products, quartz or colloidal silica and carbon sources (acetylene carbon black and phenolic resin), on the carbothermal synthesis of SiC. Finally, Ishihara [12] synthesised silicon carbide powders via sol–gel processing, beginning with fumed silica powder as the silicon source and phenolic resin as the carbon source.

Another way to decrease the temperature of the synthesis of SiC is to include the silicon and carbon atoms in the same molecule. For example, after the pyrolysis of poly(silylene)-diacetylene under inert atmosphere (1400 °C), Corriu [17] described the crystallisation of  $\beta$ -SiC: Depending on the composition of the polymer, the value of C/Si could be adjusted to produce different composites of SiC–C. The formation of a  $sp^2$ -carbon matrix surrounding the SiC particles led to efficient reduction conditions and could be used for the carbothermal reduction of other oxides. In this way, mixed-metal carbide ceramics (SiC/TiC, SiC/ZrC...) were prepared at lower temperatures, i.e. a few hundred degrees, compared to those used during the carboreduction of the parent oxides with carbon black [7]. Other authors [18–22] have described the use of carbonaceous silica gels for the synthesis of SiC.

The synthesis route and the processing conditions (the nature and size of the precursors) have a great influence on the physical characteristics of the final products [23], particularly on the surface area [1, 6, 13, 14, 16, 18, 19, 22, 24–32] (Table 1). In addition to the effect on temperature of synthesis for SiC, the different methods presented above also impact the final characteristics of the silicon carbide obtained. Overall, these methods can be classified into two categories. Direct methods consist of the reaction of the silicon oxide or the elemental silicon with solid carbon at high temperatures and lead to powders with low surface areas. In contrast, multiphase synthesis routes involve a reaction between a liquid and a gaseous phase or the pyrolysis of a gel. In this second category, the decomposition of an organic precursor leads to compounds with higher surface areas.

To quantify the influence of the nature of the precursors on their conversion temperature and on the characteristics of the final products, we have chosen to study a simple system in which the characteristics of the precursors can be modified on different scales: molecular, nanometric and, finally, micrometric. In all cases, the precursors are a mixture of carbohydrates in the form of simple ‘sugar’ and silica. In the present study, two different routes are compared for the production of silicon carbide powders. The

first, called the ‘colloidal route’, is inspired by methods used by Martin [13, 14] and consists of the carboreduction of colloidal silica (nanometric or micrometric powders) by sugar. The second route, called the ‘molecular route’, uses a molecular chemistry approach, based on the immobilisation of sugar derivatives in silica. Both synthesis routes use the same carbon source to achieve the carboreduction. The physical characteristics of the final products (surface area, grains size...) are discussed in terms of the nature of the oxide precursors (colloidal silica, fumed silica), the composition of the parent sugar (mannitol, sorbitol,  $\beta$ -cyclodextrin, sucrose) and the sugar/oxide ratio.

## Experimental

### Characterisation

Infrared spectra of the precursors and xerogels were recorded on an FT-IR Perkin-Elmer 1600 neat in KBr pellets. The  $^{29}\text{Si}$  CP MAS NMR spectra were recorded on a Bruker FTAM 300, as were the  $^{13}\text{C}$  CP MAS NMR spectra; in both cases, the repetition times were 10 and 5 s with contact times of 5 and 3 ms. The  $T^n$  and  $Q^n$  notations are given for  $[(\text{SiO})_n(\text{R})\text{SiO}_{3-n}]$  and  $[(\text{SiO})_n\text{SiO}_{4-n}]$  environments, respectively. Thermal analyses were carried out with a Netzsch STA 409 thermogravimetric analyser. The surface areas and the pore size distribution were obtained by ASAP 2020, using nitrogen gas as the adsorptive at 77 K. Before these measurements, the samples were degassed at 350 °C for 4 h under a vacuum of  $10^{-2}$  mbar. Elemental analyses of carbon and oxygen were performed by LECO CS230 and TCH600 analysers, respectively. The oxygen content in the powder was determined by combustion analysis under helium and IR detection of the  $\text{CO}_2$ -vibration. The combustion method was also used to determine the carbon content. The SiC powder was heated under an oxygen flow. Added Fe powder was used to assist the combustion. The IR detection of the  $\text{CO}_2$  formed was used again to detect the carbon content. Powder X-ray diffraction patterns were measured on a Bruker D8 advance diffractometer, using  $\text{CuK}\alpha$  radiation in the Bragg–Brentano geometry. SEM analyses were obtained with a FEI QUANTA FEG 200 ESEM environmental scanning electron microscope coupled with an EDX Bruker XFlash 4010 SDD microanalyser.

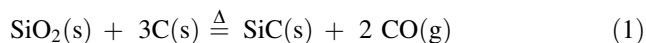
### Colloidal precursors

The overall carbothermal reduction of silica can be described as depicted in Eq. (1):

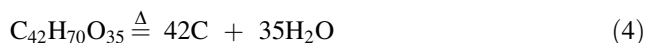
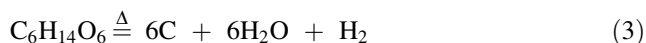
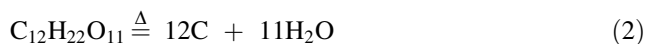


**Table 1** Bibliographic results showing the influence of synthesis parameters on the specific surface area of samples of SiC

Method	Reactions and processing conditions	S (m <sup>2</sup> /g)	Ref.
Solid state reaction	SiO <sub>2</sub> + C (1450–1550 °C)	9–23	[16]
	SiO <sub>2</sub> + C (1700–1800 °C)	6.7	[25]
	Si + C (1350 °C)	<30	[26]
Carboreduction	SiO <sub>2</sub> + sugar (1500–1800 °C)	6–30	[13–14]
	SiO <sub>2</sub> + sugar (1500–1800 °C)	115	[24]
Gas solid reaction	C + SiCl <sub>4</sub> + H <sub>2</sub> (1000 °C)	30	[28]
Pyrolysis of an organosilicon polymer	Tetramethylsilane	50	[29]
	[(C <sub>6</sub> H <sub>6</sub> )SiO <sub>1.5</sub> ] <sub>n</sub> (N <sub>2</sub> -1000 °C)	145	[30]
	TEOS + phenolic resin	112	[19]
	Polymer + silica hybrid (1000 °C-Ar/H <sub>2</sub> )	1793	[31]
	TEOS + sucrose (1100 °C-vacuum)	167	[18, 27]
	Phenyltrimethylsilane	450–620	[6]
	TEOS + alkylloxysilane (1350 °C-Ar)	151–345	[22]
	TEOS + fufuryl alcohol (1300 °C-Ar)	120–167	[32]



Several carbohydrate derivatives (sucrose, sorbitol, mannitol,  $\beta$ -cyclodextrin) were used as carbon sources. Sucrose, sorbitol and mannitol were purchased from Fisher chemical and exhibit a high purity grade (AR or ACS).  $\beta$ -cyclodextrin was purchased from Sigma-Aldrich. The pyrolysis of the carbohydrate proceeds according to the following reactions:



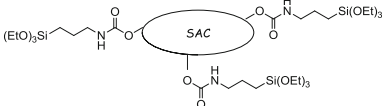
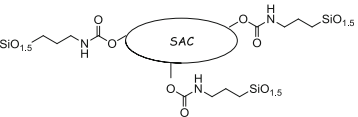
Others gaseous species are produced during the thermal decomposition of such carbohydrates [33] (CH<sub>4</sub>, C<sub>n</sub>H<sub>2n</sub>, CO<sub>2</sub>, CO), thus inducing a loss of the carbon available to be used in the carbothermal reaction (1). Silica fumed and micrometric silica was used to elaborate the silicon carbide powders. These products were purchased from Sigma-Aldrich. Fumed silica is amorphous silica with a chain-like particle morphology composed of submicron-sized spheres, which are highly branched into aggregates from 10 to 30 spheres in length, with sizes from 0.1 to 0.2  $\mu$ . The surface

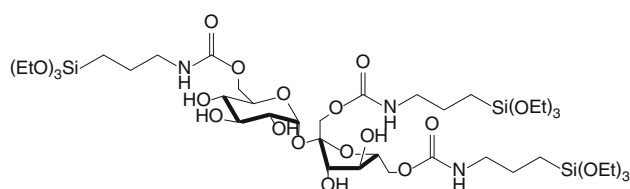
area approaches 360 m<sup>2</sup>/g, which corresponds to an effective average particle size of 7 nm. Micrometric silica powders are composed of coarse grains on the order of 1–10  $\mu$ m in size, having surface areas of approximately 6 m<sup>2</sup>/g. These oxides were mixed together with a quantity of carbohydrate derivatives (sucrose, mannitol, sorbitol,  $\beta$ -cyclodextrin) dissolved into an aqueous solution corresponding to the final composition targeted. The suspension obtained ensured a homogeneous mixing of constituents in a simple way at all scales. The amount of carbohydrate derivative present was adjusted to be between 1 and 12 times the quantity required by reaction (1) to obtain a complete conversion of the parent compounds. The atomic ratio C/Si is used to quantify the excess carbohydrate. This ratio was calculated considering the decomposition of sucrose, hexitol or cyclodextrin, according to reactions (2), (3) and (4). After complete dissolution of the sugar derivatives in the silica sol, the suspension was frozen and freeze-dried to obtain a powder. The five different precursors (P1, P2, P3, P4, P5) described in Table 2 were all obtained according to this process. The last stage, corresponding to the thermal conversion, is described in the next section of this article.

#### Molecular precursors

Thanks to the peculiar reactivity of some of the sucrose OH groups, mono- or poly-substituted products can be prepared. The preparation of sucrose carbamates (urethane) in dipolar aprotic solvents in the presence of base generally led to poly-substituted derivatives. The carbamates' formation from the reactive alcohols' functionalities of the sucrose with isocyanates was performed in anhydrous dimethylformamide which is a convenient solvent for sucrose and promotes the poly substitution; the reaction was carried out in the presence of triethylamine as a catalyst. The molecular precursor C1 (Fig. 1) based on sucrose carbohydrate was obtained according to the synthesis described below. Reagent grade 3-(triethoxysilyl)propylisocyanate was commercially available and used without purification. All reactions were carried out under argon using a vacuum line and Schlenk techniques. Solvents were dried and distilled just before use. The synthesis of this precursor consisted of two steps. First, the compound ter-[3-(triethoxysilyl)propylcarbamate]-saccharose was obtained by the reaction of 3-(triethoxysilyl)propylisocyanate with saccharose and triethylamine (precursor C1). Second, the ter-[3-(triethoxysilyl)propylcarbamate]-saccharose was subjected to hydrolysis-condensation to form a xerogel (precursor M1). This reaction occurred without adding a catalyst compared to the classical sol gel process. This phenomenon was already observed in the case of silylation of polyols [34].

**Table 2** Precursors used for silicon carbide synthesis

Carbon source	Precursor composition	Name	C/Si
Molecular route			
Sucrose		C1	14
Sucrose		M1	8
Colloidal route			
Sucrose	Fumed silica + sucrose	P1	2–36
Sorbitol	Fumed silica + sorbitol	P2	3.6
Mannitol	Fumed silica + mannitol	P3	3.6
Cyclodextrin	Fumed silica + cyclodextrin	P4	4.5
Sucrose	Micrometric silica + sucrose	P5	2–4

**Fig. 1** Possible structure for the molecular precursor C1

### Synthesis of the precursor C1

To a solution of 2 g (5.84 mmol) of saccharose in dry DMF (20 ml) at 90 °C under argon, 1.77 g (17.5 mmol) of freshly distilled triethylamine and 4.33 g (17.5 mmol) of 3-(triethoxysilyl)propylisocyanate were added. The mixture was stirred at 90 °C for 7 days. The solvent was then removed under vacuum for 32 h at room temperature. The resulting oil was coevaporated with dry toluene several times to obtain a brown solid. This solid was washed with heptane then dried to obtain 5.5 g (87 %) of desired product C1 with a small amount of polycondensed product. As its solubility was very low in any solvent, C1 was analysed as a solid.<sup>1</sup> The <sup>13</sup>C solid state NMR for C1 exhibits the characteristic resonance of the precursor, the resonance at 156 ppm was attributed to the carbamate resonance, whilst the presence of a peak around 58 ppm (CH<sub>2</sub>–O) and 18 ppm (CH<sub>3</sub>) indicates that the alkoxy group has been successfully introduced; this was also confirmed with the resonance at 7 ppm corresponding to a

carbon atom covalently bonded to silicon. The spectrum exhibits additional signals attributed to the sucrose in the region between 20 and 100 ppm. The IR spectra showed the expected peaks in agreement with the composition of the precursor with the specific band corresponding to the carbamate at around 1700 ( $\nu_{\text{CO}}$ ) and 1530  $\text{cm}^{-1}$  ( $\delta_{\text{NH}}$ ); in addition, no NCO peak corresponding to isocyanate was observed at around 2300  $\text{cm}^{-1}$ .

The elemental analysis confirms the polysubstitution of the sucrose, the result concordant with the introduction of 3 (triethoxysilyl)propylcarbamate functionalities.

### Synthesis of the xerogel M1

A suspension of 1 g (0.92 mmol) of ter-[3-(triethoxysilyl)propylcarbamate]-saccharose in technical ethanol (15 ml) was stirred at 110 °C for 24 h, then kept without stirring for 48 h. The reaction mixture was then cooled at room temperature and concentrated for 7 days. The resulting xerogel was filtered and washed with ethanol, followed by Soxhlet extractions with ethanol (15 h) then acetone (15 h). The final solid was dried under vacuum to give 0.551 g (79 %) of pale brown powder.<sup>2</sup> The sucrocarbamate looks stable with regard to the sol–gel reaction (reflux in ethanol with traces of water) and to the treatment; this was confirmed with the persistence of the amide characteristic peaks in the solid state NMR spectrum at

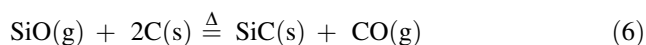
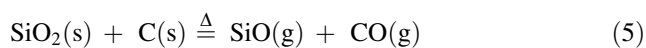
<sup>1</sup> Elem. Anal. Found: C, 41.97; H, 6.82; N, 3.93; O, 35.3; Si, 8.90. Calc. for C<sub>42</sub>H<sub>85</sub>N<sub>3</sub>O<sub>23</sub>Si<sub>3</sub>: C, 46.52; H, 7.90; N, 3.88; O, 33.97; Si, 7.77. FTIR  $\nu_{\text{max}}/\text{cm}^{-1}$  3334, 2973, 2927, 2886, 1699, 1531, 1444, 1246, 1056, 949; <sup>13</sup>C CP MAS NMR 75 MHz ( $\delta$ , ppm) 156.9, 103.2, 90.2, 71.7, 58.1, 43.5, 23.2, 18.2, 7.7. <sup>29</sup>Si CP MAS NMR 60 MHz ( $\delta$ , ppm): –45.1 (T<sup>0</sup>), –52.8 (T<sup>1</sup>). Level of condensation <12 %.

<sup>2</sup> Elem. Anal. Found: C, 35.43; H, 5.43; N, 4.48; O, 37.7; Si, 10.01. Calc. for C<sub>48</sub>H<sub>80</sub>N<sub>6</sub>O<sub>37</sub>Si<sub>6</sub>: C, 38.39; H, 5.37; N, 5.60; O, 39.4; Si, 11.22. FTIR  $\nu_{\text{max}}/\text{cm}^{-1}$  3330, 2934, 2360, 2335, 1693, 1528, 1001, <sup>13</sup>C CP MAS NMR 75 MHz ( $\delta$ , ppm) 158.7, 104.9, 92.1, 73.5, 63.6, 44.4, 24.6, 11.2. <sup>29</sup>Si CP MAS NMR 60 MHz ( $\delta$ , ppm): –57.4 (T<sup>2</sup>), –64.4 (T<sup>3</sup>). Level of condensation >95%. BET surface area <10 m<sup>2</sup> g<sup>–1</sup>.

around 159 ppm and by FT-IR with the vibration band at around 1700 and 1530  $\text{cm}^{-1}$ . Furthermore, the elemental analysis suggests that the 3 (triethoxysilyl)propylcarbamate functionalities were kept after the sol-gel process. Beside the persistence of the carbamate group, the polycondensation of the alkoxy groups of the molecular precursor C1 was followed by NMR and FT-IR. The  $^{13}\text{C}$  solid state NMR for M1 showed the disappearance of the peaks at 58 and 18 ppm, which indicates the complete hydrolysis of the alkoxy groups, and the characteristic signal of the precursor with the resonance at 14 ppm corresponding to the carbon atom covalently bonded to silicon confirms that no carbon-silicon cleavage has occurred during the hydrolysis and condensation reactions.  $^{29}\text{Si}$  NMR spectra exhibited  $\text{T}^2$  [ $\text{C}-\text{Si}(\text{OSi})_2(\text{OH})$ ] and  $\text{T}^3$  [ $\text{C}-\text{Si}(\text{OSi})_3$ ] units with a majority of  $\text{T}^3$ . The degree of condensation of the silicate networks was evaluated and found superior at 95 %; the absence of Q units confirmed that no C-Si cleavage occurred during the hydrolysis. The extent of condensation was suggested with the IR spectra with the broadening of the band located at around 1000–1100  $\text{cm}^{-1}$  confirming the Si-O-Si network formation.

#### Pyrolysis of the precursors

After the different syntheses presented above, the precursors were obtained as white, beige or brown ceramic powders, depending on the routes chosen. In the first step, the powders (Pn, M1 and C1) could be compacted to obtain a better confinement of the silica by the surrounding carbohydrate derivative. In the second step, the compacts were preheated at 800 °C for 3 h under argon flow to facilitate the complete decomposition of the carbohydrate derivative into carbon. Then, the formation of SiC was carried out at higher temperatures (1100–1550 °C) for 4 h under argon flow. It has been suggested that, under reduction conditions, silica leads to the formation of the gaseous SiO species [13]. Thus, the carbothermal reduction of silica can be described as follows:



Pressure and temperature have been used by several authors to control the reaction kinetics. A dynamic vacuum was employed by Zeng [18] to decrease the temperature of the carbothermal reaction to 1100 °C; this parameter was not investigated in this work. Most of the syntheses are carried out at temperatures above 1400 °C under argon flow. Under these conditions, reactions (5) and (6) become predominant [16]. Experimentally, the condensation of silica, indicating the presence of SiO gas, was observed in the furnace after pyrolysis of the samples.

The conversion of the ceramic precursors was carried out in a tubular furnace and in the TGA apparatus. A flow of argon over 30 l/h was used in the tubular furnace to evacuate the gaseous species produced during the thermal treatment. For the samples treated in the TGA apparatus, the argon flow was lower than 20 ml/min, leading to an incomplete conversion. The products obtained exhibited colours ranging from grey-blue to black, depending on the excess of carbohydrate derivative added.

#### Results

Various carbohydrate derivatives (sucrose, manitol, sorbitol,  $\beta$ -cyclodextrin) and silica of different grain sizes (micrometric and nanometric) were used for the synthesis of the carbide precursors (see Table 2). The C/Si ratio depends on the initial number of silicon and carbon atoms in the different precursors (molecular, colloidal or micrometric). The ratio C/Si was increased up to 36 for P1-type precursor (sucrose + fumed silica) because the resulting material presented interesting features, i.e. mesoporosity and high surface area (see Sect. 3.2). This ratio cannot be changed significantly in molecular precursors C1 and M1 and was not much change with P2-, P3-, P4- and P5-type precursors.

#### Silicon carbide formation

A C/Si ratio higher than 3 was necessary to obtain single-phase SiC after the heat treatment at 1550 °C of the P1-type precursors (sucrose + fumed silica). This result was surprising because a part of the silica was converted to gaseous SiO, according to reactions (5) and (6), and because a part of the carbon was lost due to the breakdown of sucrose into gaseous species, e.g. CO, CO<sub>2</sub>, CH<sub>4</sub> and alkenes. It can be concluded that these two antagonistic phenomena seem to compensate for each other. This result is consistent with those of Martin [13, 14] and Cerovic [24]. The main phase detected by XRD in these conditions was the cubic phase ( $\beta$ -SiC) (Fig. 2); however, a shoulder was observed on the XRD pattern at the position  $33.5^\circ < 2\theta < 34.5^\circ$ . This indicates the presence either of a low amount of  $\alpha$ -SiC or of some stacking faults in the sample. Below the ratio C/Si = 3, cristobalite was detected by XRD; in parallel, the oxygen content was determined to be very high (16.6 wt%) (see supplementary information section), indicating the presence of silica in the sample. For a value of C/Si higher than 9, a broad peak was detected at the position  $20^\circ < 2\theta < 28^\circ$  as a consequence of the presence of amorphous carbon in the sample (Fig. 2). Elemental analysis jointly confirmed this point and the decrease in the amount of oxygen in the final products to

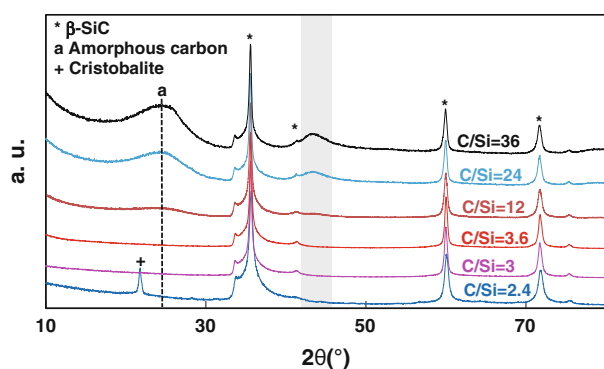


**Fig. 2** X-ray diffraction pattern of heat-treated precursor P1, fumed silica + sucrose, (1550 °C—4 h) versus the ratio C/Si. Grey area in this figure is an artefact corresponding to the signal of the sample holder used to analyse the powders

0.4 wt% for the ratio C/Si = 36. Elemental analysis is more sensitive than XRD analysis in the detection of free carbon.

The evolution of the X-ray patterns is shown as a function of temperature in Fig. 3. The formation of silicon carbide occurred for temperatures close to 1300 °C. After reacting at 1250 °C, the sample was completely amorphous, and no crystalline phase was detectable by X-ray diffraction; the sample most likely consists of only silica and carbon. Otherwise, the reaction was complete at 1450 °C. More precisely, TGA analysis shows that the reaction started when the temperature reached 1300 °C and ended when the temperature reached 1550 °C (Fig. 4). This result is consistent with the literature (Table 1). The evolution of the oxygen content in the samples versus the temperature of the heat treatment is another way to follow the progress of the carbothermal reaction. This parameter decreased to a value of 1.1 wt% when the temperature increased to 1550 °C (Fig. 5).

Conversely, pyrolysis in the same conditions as the precursors P2 (fumed SiO<sub>2</sub> + sorbitol) and P3 (fumed

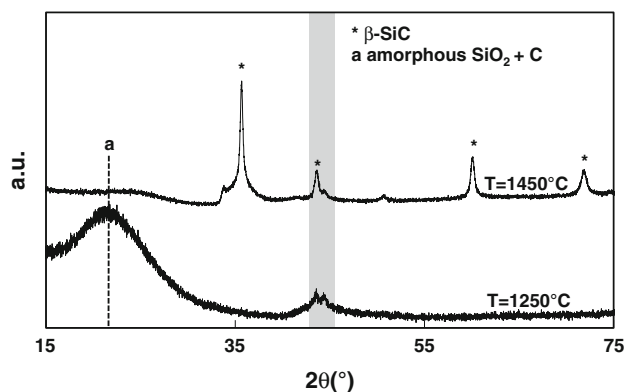


**Fig. 3** X-rays patterns of heat-treated precursor P1, fumed silica + sucrose C/Si = 12, versus the pyrolysis temperature for a dwell time of 4 h. Grey area in this figure is an artefact corresponding to the signal of the sample holder used to analyse the powders

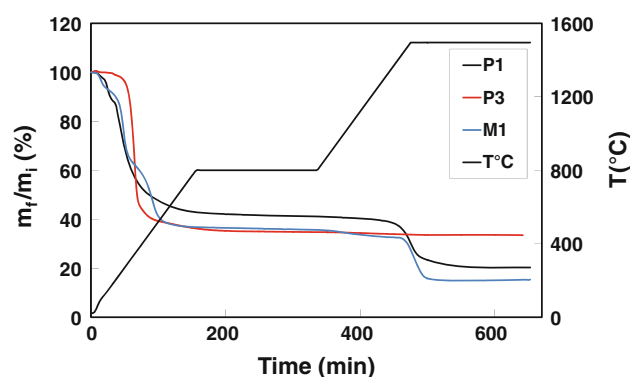


**Fig. 4** TGA curves (in argon) of precursors P1 (fumed silica + sucrose C/Si = 3.6), P3 (fumed silica + mannitol C/Si = 3.6), M1 (molecular route, C/Si = 8)

SiO<sub>2</sub> + mannitol) led to the formation of cristobalite and a small amount of β-SiC (Fig. 6). This result can be attributed to the evaporation of a portion of these two carbohydrates when they reached their boiling points (296 and 290 °C for sorbitol and mannitol, respectively) [35], which led to a precursor with a deficit of carbon relative to the reaction (1). Unlike mannitol or sorbitol, sucrose and cyclodextrin decompose into carbon and gaseous species [33] at low temperatures (<800 °C), and the remaining carbon is efficient for the carbothermal reduction of the silica at a high temperature (>1300 °C). TGA (Fig. 4) confirmed this point.

The conversion of the precursor type P5 into silicon carbide was comparable to that of the precursor P1. However, for the same value of the ratio C/Si, the oxygen content was higher in powders made from micrometric silica, presumably due to their lower reactivity during the carbothermal reduction.

The doping of sol–gel matrices with organic molecules via the simple mixture of organic and inorganic matrices is one of the simplest ways to entrap organic molecules in an

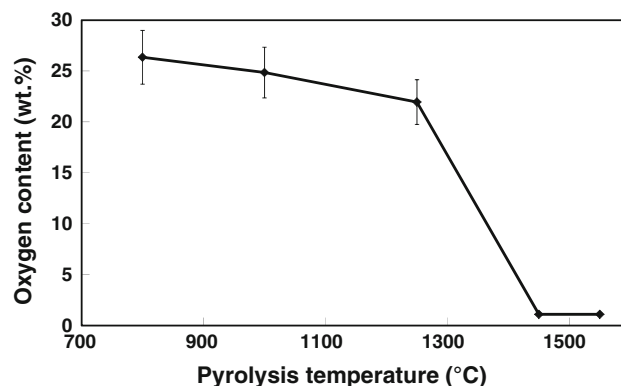


**Fig. 5** Oxygen content of samples P1 (fumed silica + sucrose C/Si = 12) versus the temperature for a dwell time of 4 h of the heat treatment



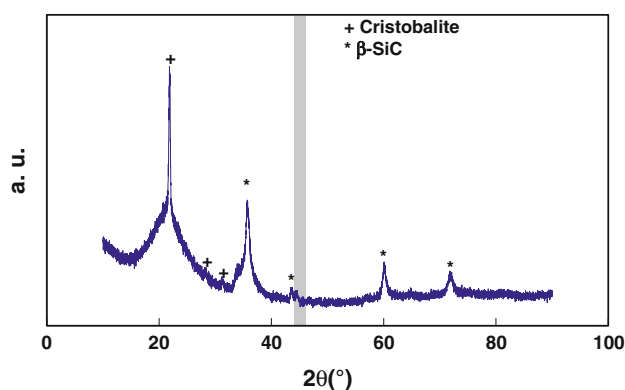


**Fig. 6** X-ray diffraction pattern of heat-treated precursor C1 (molecular route) and P3 (fumed silica + mannitol) at 1550 °C—4 h. Grey area in this figure is an artefact corresponding to the signal of the sample holder used to analyse the powders

inorganic network [36]. The adjustment of the C/Si ratio is straightforward. However, because weak interactions between the organic and inorganic matrices are related to the dispersion of the organic fragment within the structure, lack of control over the distribution is a major drawback as segregation can occur easily.

The dynamic segregation into two coexisting phases may have an impact during the preparation of silicon carbide; the covalent approach in the molecular route can be employed to overcome this drawback. Moreover, the molecular route allows the formation of a hybrid organic–inorganic material, where the silicon atom is already covalently bonded to the carbon atom. This may influence the temperature of the formation of silicon carbide. The molecular precursor C1, the carbon source of which is not embedded in the silica matrix, can be used directly in the preparation of SiC with a theoretical C/Si ratio value equal to 14 ( $C/Si = 11.6$  from the elemental analysis). The hydrolysis-condensation of bis or tris(trialkoxysilyl) organic molecules led to hybrid organic–inorganic silica with covalent linkages between the organic and the silicate network. Bridged organo-polysilsesquioxanes can be obtained directly from the hydrolysis-condensation reaction of C1, ultimately leading to a type II hybrid material M1. These organo-polysilsesquioxanes consist of highly condensed siloxane networks with organic fragments covalently bonded to the silica network (level of condensation >95 % estimated by  $^{29}\text{Si}$  solid state NMR from the  $T^2$  and  $T^3$  silicate centres). This approach leads to a final material M1 with a theoretical ratio C/Si equal to 8.

In our study, the preparation of silicon carbide by the ‘molecular route’ was investigated with the precursors C1 (molecule) and M1 (Xerogel), having theoretical C/Si ratios equal to 14 and 8, respectively. The pyrolysis of these two precursors (C1 and M1) at 1550 °C led to the formation of  $\beta$ -SiC (Fig. 7).

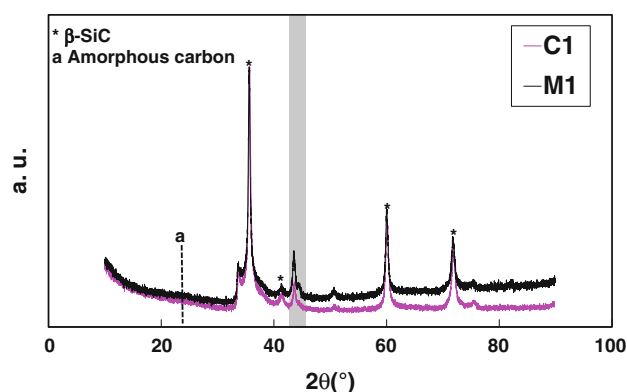


**Fig. 7** X-ray diffraction pattern of heat-treated precursors C1 and M1 (molecular route) at 1550 °C—4 h. Grey area on this figure is an artefact corresponding to the signal of the sample holder used to analyse the powders

Let us now consider the transformation of the molecular precursor M1 into silicon carbide. After the pyrolysis of the precursor at 1100 °C, XRD analysis shows no evidence of crystalline silica or other crystalline compounds. However, Si, O and C were principally detected by EDX microanalysis, and elemental analyses confirm the presence of oxygen, residual nitrogen and carbon arriving from the decomposition of the starting products. These observations can be interpreted to signify the presence of amorphous silica and amorphous carbon within the sample, and it can be concluded that the mechanism of the formation of silicon carbide from these molecular precursors is similar to that observed with colloidal precursors. In the first temperature domain, up to 1000 °C, the product decomposes into C and  $\text{SiO}_2$ ; for temperatures higher than 1300 °C, carbothermal reduction occurs. Nevertheless, TGA analysis of the M1 precursor presented in Fig. 4 is consistent with the mechanism of the formation of SiC described for the colloidal precursors.

#### Characterisation of the samples

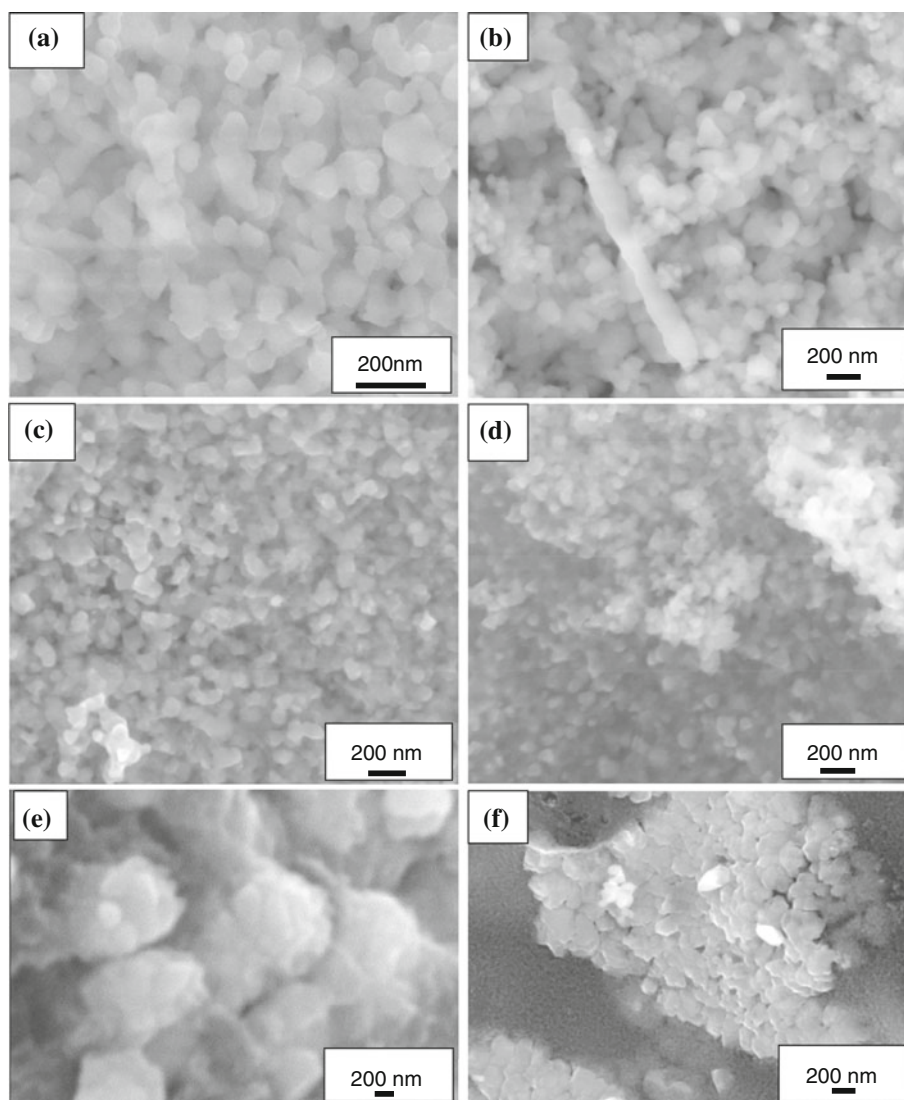
SEM was employed to observe the morphology of SiC particles synthesised with various C/Si ratios. SEM observations reveal a similar crystallite size ( $\approx 80$ –150 nm) of the powders elaborated from the colloidal route with the precursors P1 (fumed  $\text{SiO}_2$  + sucrose) and P4 (fumed  $\text{SiO}_2$  +  $\beta$ -cyclodextrin) for a C/Si ratio close to 4 (Fig. 8a, b). In contrast, the particles obtained from the micrometric silica, precursor P5, agglomerated with a characteristic size greater than 1  $\mu\text{m}$ . This was particularly clear for samples having a C/Si ratio = 24. However, these particles are composed of smaller crystallites  $\approx 300$ –500 nm (Fig. 8f). When the C/Si ratio increases, the amount of the carbon matrix increases and the microstructure of the powders becomes more heterogeneous for all the samples. The size of

the agglomerates in the P1-type samples (fumed silica + sucrose) was approximately 700–1000 nm, and the size of the constitutive crystallites was approximately 200 nm (Fig. 8e). SEM observations of the powders elaborated from the precursors M1 and C1 (molecular route) reveal particles with lower crystallite sizes, typically 70–100 nm (Fig. 8c, d). The difference in the crystallite size is a consequence of the better homogeneity of such materials. The size of the SiC crystallites obtained from the Scherrer formulae, for the precursors P1, P4, M1 and C1 pyrolysed at 1550 °C, is in the range of 15–30 nm. This value is lesser than the value obtained by the SEM observations, i.e. 80–150 and 70–100 nm. Such results indicate that the particles observed by SEM are constituted by aggregation of smaller ‘coherent diffraction domains’.

The specific surface area ( $S_{\text{BET}}$ ) of the various samples that pyrolysed at 1550 °C is plotted versus the C/Si ratio in Fig. 9. This final specific surface area is strongly dependent

on the nature of the precursor. The evolution of the surface area of the materials P1 (fumed silica + sucrose) versus C/Si is characterised by 4 domains. For a C/Si ratio lower than 3, the final product is a mixture of cristobalite + SiC. Therefore, the surface area decreases as a consequence of the sintering of the fumed silica grains. Uchino [37] measured a decrease in the surface areas of fumed silica heat treated at 1000, 1100 and 1200 °C, from 188 to <1 m<sup>2</sup>/g. In the second range, i.e. for initial values of C/Si ranging from 3.6 to 6, the transformation of silica into single-phase SiC was complete. The surface area varied moderately; it was representative of the outer surface of the SiC crystallites formed. The SiC crystallites observed by SEM had a characteristic size of approximately 100 nm (Fig. 8a). The value of the diameter of the particle,  $d = 125$  nm, estimated from the surface area measurement by assuming that the SiC particles are spherical, is in good agreement with this observation, i.e.  $d = 6000/(\rho S)$ , where  $\rho$  is the density

**Fig. 8** SEM micrograph of **a** P4 fumed silica +  $\beta$ -cyclodextrin C/Si = 4.5, **b** P1 fumed silica + sucrose C/Si = 3.6, **c** M1 molecular precursor C/Si = 8, **d** C1 molecular precursor C/Si = 14, **e** P1 fumed silica + sucrose C/Si = 24, **f** P5 micrometric silica + sucrose C/Si = 24 after pyrolysis at 1550 °C—4 h under argon



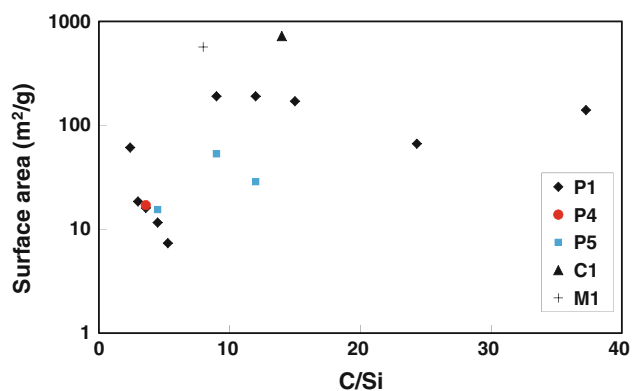


**Fig. 9** Specific surface area (BET) of carbides elaborated from various precursors versus the ratio C/Si (processing conditions 1550 °C—4 h under Ar). (P1 fumed silica + sucrose, P4 fumed silica +  $\beta$ -cyclodextrin, P5 micrometric silica + sucrose, C1 molecular precursor, M1 hybrid xerogel)

of SiC (3.2 g/cm<sup>3</sup>) and the surface area  $S$  is 15 m<sup>2</sup>/g. In the third domain, a sharp increase was observed in the surface area for samples with values of C/Si between 6 and 12. SEM observations revealed the presence of a much more important matrix of porous carbon that coated the SiC grains. This was the consequence of the large amount of residual carbon. No significant change was observed in the grain size of the SiC crystallites (200 nm), confirming that the porosity was located in the carbon matrix surrounding the silicon carbide grains. The maximum surface area developed by this material (200 m<sup>2</sup>/g) was one order of magnitude greater than the outer surface that would be developed (10 m<sup>2</sup>/g) by powders with a grain size of 200 nm alone. This confirms the hypothesis that the location of the porosity is in the matrix of residual carbon. Finally, for values of C/Si ranging from 12 to 36, the specific surface area of the powders decreased to values near the surface area of sucrose (1 m<sup>2</sup>/g) pyrolysed under the same conditions. In contrast, materials made from micrometric silica + sucrose (P5) had low specific surface areas, even when they had high residual carbon content (Table 2). This difference will be discussed in the next section which addresses the mechanism of porosity formation within these powders. Finally, it is clear that the molecular route did not offer much flexibility in the variation of the C/Si ratio in the sample. Therefore, the only points of comparison between the molecular and the colloidal routes were obtained for values of C/Si equal to 8 and 14. The specific areas of such materials were the highest obtained in this study, i.e. 722 m<sup>2</sup>/g for C1 and 567 m<sup>2</sup>/g for M1, and the morphology of their particles did not present any intra-particle porosity. The surface areas of the samples C1 and M1 were nearly the same, which was consistent with the final amount of carbon measured on these samples after heat treatment at 1550 °C. This result

can be explained by the fact that although the value of C/Si was higher in the precursor C1, the alkoxy groups associated with the silicon were removed at low temperatures and were not operative for the carbothermal reaction. The grain sizes of the SiC particles after the pyrolysis of the molecular precursor were close to 70–100 nm; we can therefore conclude, as for the precursors of type P1 (fumed silica + sucrose), that the porosity is located in the residual carbon phase.

## Discussion

### Effect of the synthesis route on the temperature of carboreduction

The first goal of this study was to evaluate the influence of the route used for the synthesis of silicon carbide on the temperature of carboreduction. Regardless of the synthesis route, two significant mass losses were observed (Fig. 4) during the pyrolysis of the precursors P1 (fumed SiO<sub>2</sub> + sucrose) and M1 (molecular route). The first loss, observed at temperatures below 800 °C, corresponds to the decomposition of the organic precursors. The second loss, which was observed for temperatures ranging from 1300 to 1500 °C, can be attributed to the formation of carbides. In the molecular route, the silica resulting from the decomposition of the precursor was associated with a highly cross-linked carbon network, which could be suitable for its carboreduction; in contrast, the reactants were mixed together at the nanometric (P1) or micrometric (P5) scale for the colloidal route. In all cases, no evidence of a temperature change was observed relative to the nature of the precursors. The carboreduction still began at a temperature near 1300 °C. The temperature of the carboreduction for the precursor P5 was not identified by TGA analysis, but furnace pyrolysis conducted at 1550 °C clearly showed a complete conversion of the precursor to  $\beta$ -SiC.

In terms of temperature conversion, our results are similar to those obtained by Corriu [38] in the case of the pyrolysis of Poly(dimethylsilylene)diacetylene. In this work, the formation of  $\beta$ -SiC was observed after the pyrolysis of the organosilicone polymer at a temperature of 1400 °C. However, the mechanism leading to the conversion of this polymer into a ceramic was different. In the range of 400–800 °C, the thermal decomposition of the organosilicone polymer led to the formation of an amorphous SiC embedded in a cross-linked carbon network resulting from the decomposition of the diacetylene groups. Finally, in the work of Corriu, the formation of  $\beta$ -SiC was observed after heat treatment at 1400 °C. The main difference between the work of Corriu and this work was the presence of oxygen in our compounds, which led to the

formation of silica during the decomposition of the precursors and led to a classical carbothermal reduction in the same way as if we had used a precursor oxide.

The results obtained in this study confirm that there is no effect caused by the size or nature of the precursors on the temperature of carbothermal reduction. This result may seem surprising because chemical Si–C links are already present within the molecular precursor. In fact, during heat treatment, these precursors are first transformed into oxides before undergoing carboreduction. However, the use of these two synthesis routes produces a relative decrease in the carboreduction temperature compared to conventional carboreduction, via the Acheson process, which relies on a conversion temperature above 2000 °C. This difference can be attributed to the molecular intimacy of the SiO<sub>2</sub>/C mixture. In this case, the reaction is not limited by the diffusion process of species in the solid state as is the case in the Acheson process. This peculiarity has also been discussed by Cerovic [24].

Finally, the synthesis of carbides by the colloidal route offers more flexibility than the molecular route to convert the precursors; indeed, it can be easy to adjust the C/Si ratio and, thus, to have better control of the composition of the sample. However, it may be possible to increase the amount of silicon in the molecular precursor to some extent by adding tetraethyl orthosilicate (TEOS) during the sol-gel process.

#### Formation of the mesoporous structure

The evolution of the specific surface areas of all the materials created from the various precursors (C1, M1, P1 and P5) is illustrated as a function of the volume fraction of carbon in Fig. 10. The volume fraction of carbon is inferred from the results of the chemical analysis of this element by assuming that the final material consists of only 2 phases, SiC and carbon.

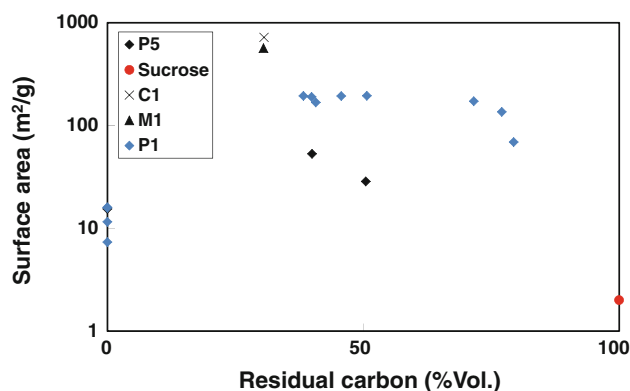


**Fig. 10** Specific surface area versus residual carbon volume fraction after the pyrolysis at 1550 °C under Ar of samples P1, P5, C1, M1 and sucrose

As shown in this figure, the nature of the precursor has a significant impact on the final specific surface area. The largest surface area was obtained for the C1 sample created from the molecular precursor (722 m<sup>2</sup>/g), whereas the samples P1 (fumed silica + sucrose) had an intermediate surface (200 m<sup>2</sup>/g) and the samples P5 (micrometric silica + sucrose) presented the lowest values. The specific surface areas of P1-type materials (fumed silica + sucrose) increased up to 200 m<sup>2</sup>/g for a volume fraction of carbon close to 50 % and then decreased to reach the surface area of sucrose pyrolysed at 1550 °C. The adsorption–desorption isotherm of the sample P1 (C/Si = 12) (Fig. 11) underwent an abrupt change when the relative pressure was in the medium range, from 0.6 to 0.9; this is a salient characteristic of mesoporous materials. The shapes of the isotherms and the hysteresis loop obtained suggest the presence of mesoporous domains in the matrix of residual carbon.

The evolution of the specific surface area versus the volume fraction of carbon can be interpreted as a consequence of the release of CO gas during the carbothermal process at higher temperatures. Further investigations were performed on the evolution of the surface area versus the pyrolysis temperature for the P1 samples (fumed silica + sucrose) at a fixed C/Si ratio = 12 (see Table 1). After pyrolysis at 800 °C, the powders showed a high surface area, close to 256 m<sup>2</sup>/g, which is very similar to the surface area of the fumed silica. As the pyrolysis temperature increased to 1250 °C, the surface area progressively decreased to 4 m<sup>2</sup>/g due to the sintering of the surrounding carbon matrix. Above 1300 °C, the gaseous species produced by the carboreduction between the silica and the carbon caused the formation of mesoporosity, which greatly increased the surface area of the powders. The same effect was observed for the pyrolysis of the molecular precursor; after pyrolysis at 1150 and 1550 °C, the surface

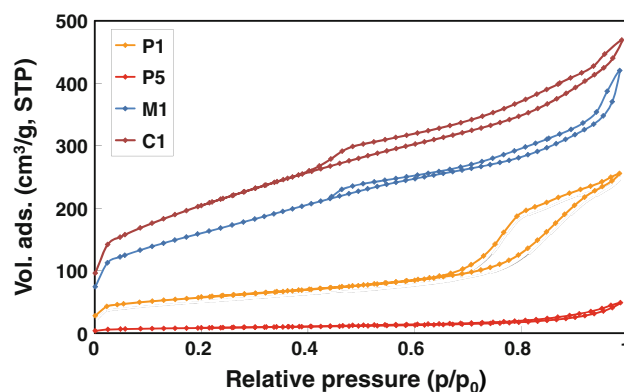


**Fig. 11** Adsorption–desorption isotherm of P1 fumed silica + sucrose (C/Si = 12), P5 micrometric silica + sucrose (C/Si = 12), M1 and C1 molecular precursors, after the pyrolysis at 1550 °C



areas were 170 and 722 m<sup>2</sup>/g, respectively. For low volume fractions of residual carbon under these conditions, SiC grains are bonded together by a thin layer of amorphous carbon, and gases produced during carboreduction can percolate via the interstices between these grains. As the volume fraction of carbon increases, the gases produced by the carbothermal reaction escape from the samples by creating narrow channels through the carbon matrix, which increase the surface area of the material. For high values of carbon content, there is not enough gas produced by the carbothermal reaction, and the surface area and the porosity volume decrease.

All these mechanisms are sketched schematically in Fig. 12, which summarises the core of the mechanisms for porosity control as proposed in this paper. The porosity of excess porous carbon is not a drawback of the routes proposed here, but it can be used to synthesise nanocomposite carbides with this second ‘external’ network of highly reactive porous carbon.

The determination of pore size distribution calculated with the BJH model from adsorption–desorption isotherms of nitrogen indicates that the characteristic diameter of the mesoporosity is smaller for the sample derived from the pyrolysis of the molecular precursor than that obtained after the pyrolysis of the colloidal precursor (Fig. 13). The pore volume of this material was also higher, which explains the large difference in surface area occupied by these materials. The size of the pore seems to be related to the size of the silica particles; in these conditions, the material prepared from the molecular precursors has better characteristics.

In contrast, the P5-type samples (micrometric silica + sucrose) exhibited the lowest specific surface area. For these samples, the silica particles agglomerated in clusters, the characteristic size of which was one micrometre. We suggest that these silica particles are much less dispersed in the sample volume, and therefore the channels created by the release of the gaseous species during the

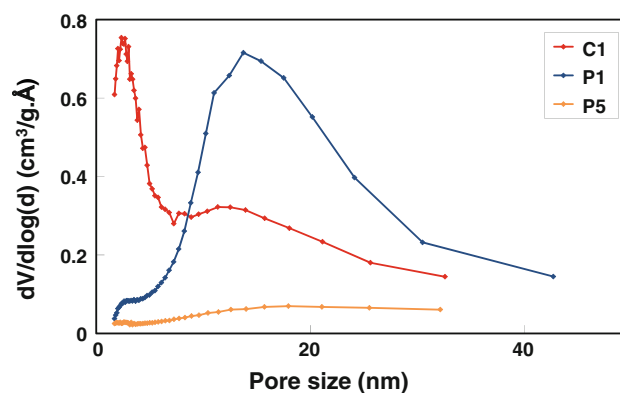


**Fig. 13** Pore size distribution (BJH) of P1 fumed silica + sucrose (C/Si = 12), P5 micrometric silica + sucrose (C/Si = 9) and C1 molecular precursor (C/Si = 14)

carbothermal reaction are larger, leading to a material with a lower specific surface area.

## Conclusion

Two different synthesis routes were used for the production of nanocrystalline carbon/ $\beta$ -SiC composite powder. The colloidal route consists of the carboreduction of colloidal silica by sugar (sucrose, mannitol, sorbitol, cyclodextrin) at high temperatures. The molecular route uses a molecular chemistry approach based on the immobilisation of polycarbosilane in sugar via a sol–gel process, which leads to the formation of  $\beta$ -SiC after high temperature conversion. In both cases,  $\beta$ -SiC powders with a high yield of submicrometric particles were successfully synthesised in the temperature range between 1300 and 1550 °C. The powders obtained by the two routes exhibited a mesoporous structure. The structure of these materials was composed of grains of carbides embedded in a matrix of carbon. Their characteristics depend on the amount of residual carbon and the mesoporosity is located within the carbon matrix

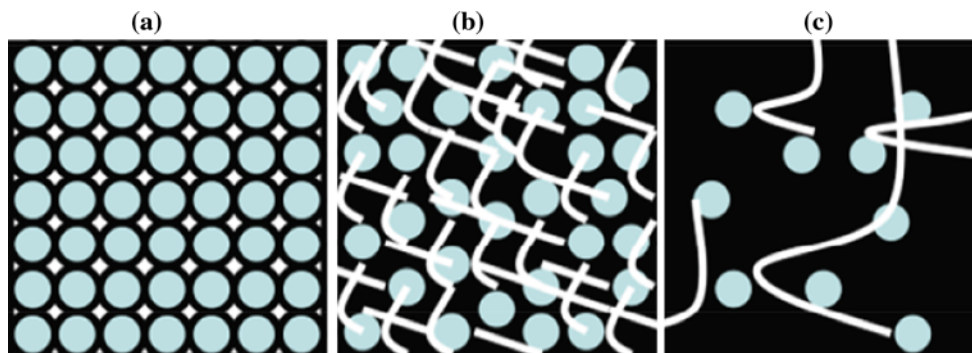


**Fig. 12** Schematic representation of the overall composition due to the carbothermic reduction of silica for samples obtained after the pyrolysis of precursors P1. Blue dots represent the domains of SiC,

whilst black represents domains made from excess carbon and showing mesoporosity (Color figure online)

surrounding the carbide grains. The largest surface area, 722 m<sup>2</sup>/g, was measured for a sample synthesised via the molecular route. A mechanism related to the release of the CO gas produced during the carbothermal reduction was proposed to explain the evolution of the surface area versus the volume fraction of residual carbon.

It may prove interesting to apply and study these synthesis routes on other novel porous carbon materials in future work. The molecular route seems to be the best way to increase the surface area of the material, and in future studies, we will evaluate the effect of polymerisation of the silica network on this parameter.

**Acknowledgements** The authors thank the GNR MATINEX, common to CNRS and CEA, for its financial support as well as M. Georges for his work on the molecular route. The authors also thank the COST network D43 and CM1011 for allowing discussions of all aspects of preparing nanomaterials during annual meetings.

## References

- Ledoux MJ, Pham-Huu C (2001) *Cattech* 5:226
- Okada K, Kato H, Nakajima K (1994) *J Am Ceram Soc* 77:1691
- Pham-Huu C, Bouchy C, Dintzer T, Ehret G, Estournes C, Ledoux MJ (1999) *Appl Catal A* 180:385
- Bao X, Nangrejo MR, Edirisinghe MJ (2000) *J Mater Sci* 35:4365. doi:[10.1023/A:1004805023228](https://doi.org/10.1023/A:1004805023228)
- Acheson EG (1893) U.S. Patent 492
- Gupta P, Wang W, Fan LS (2004) *Ind Eng Chem Res* 43:4732
- Corriu RJP (2000) *Angew Chem Int Ed* 39:1376
- Roduner E (2006) *Chem Soc Rev* 35:583
- Koga K, Ikeshoji T, Sugawara K (2004) *Phys Rev Lett* 92:115507
- Kevorkijan VM, Komac M, Kolar D (1992) *J Mater Sci* 27:2705. doi:[10.1007/BF00540693](https://doi.org/10.1007/BF00540693)
- Lin YJ, Tsang CP (2003) *Ceram Int* 29:69
- Ishihara S, Tanaka H, Nishimura T (2006) *J Mater Res* 21:1167. doi:[10.1557/jmr.2006.0138](https://doi.org/10.1557/jmr.2006.0138)
- Martin HP, Ecke R, Muller E (1998) *J Eur Ceram Soc* 18:1737
- Martin HP, Muller E, Knoll Y, Strienitz R, Schuster G (1995) *J Mater Sci Lett* 14:620
- Julbe A, Larbot A, Guizard C, Cot L, Charpin J, Bergez P (1990) *Mater Res Bull* 25:601
- Krstic VD (1992) *J Am Ceram Soc* 75:170
- Corriu RJP, Gerbier P, Guerin C, Henner B (1992) *Angew Chem Int Ed* 31:1195
- Zheng Y, Wang R, Wei RKW (2008) *J Mater Sci* 43:5331. doi:[10.1007/s10853-008-2778-8](https://doi.org/10.1007/s10853-008-2778-8)
- Jin GQ, Guo XY (2003) *Micropor Mesopor Mater* 60:207
- Colombo P, Mera G, Riedel R, Soraru GD (2010) *J Am Ceram Soc* 93:1805
- Babic B, Bucevac D, Radosavljevic-Mihajlovic A, Dosen A, Zagorac J, Pantic J, Matovic B (2012) *J Eur Ceram Soc* 32:1901
- Xu J, Liu YM, Xue B, Li YX, Fan KN (2011) *Phys Chem Chem Phys* 13:10111
- Ohji T, Fukushima M (2012) *Int Mater Rev* 57:115
- Cerovic L, Milonjic SK, Zec SP (1995) *Ceram Int* 21:271
- Wei GCT (1983) *J Am Ceram Soc* 66:C111
- Larpiattaworn S, Ngerchuklin P, Khongwong W, Pankurdee N, Wada SW (2006) *Ceram Int* 32:899
- Shen XN, Zheng Y, Zhan YY, Cai GH, Xiao YH (2007) *Mat Lett* 61:47666
- Moene R, Makkee M, Moulijn JA (1998) *Appl Catal A* 167:321
- Vannice MA, Chao YL, Friedman RM (1986) *Appl Catal* 20:91
- Lednor PW (1992) *Catal Today* 15:243
- Li FB, Qian QL, Zhang SF, Yan F, Yuan GQ (2007) *J Nat Gas Chem* 16:363
- Wang DH, Fu X, Jin GQ, Guo XY (2011) *Int J Mater Res* 102:1408
- Tomasik P, Palasinski M, Wiekak S (1989) *Adv Carbohydr Chem Biochem* 47:203
- Hérault D, Rodembusch FLC, Gingras M, Cerveau G, Corriu RJP (2010) *C R Chimie* 13:566
- Deschanel X, Delchet C, Hérault D, Magnin V, Podor R, Cerveau G, Zemb T, Corriu R (2010) *Prog Colloid Polym Sci* 137:47
- Avnir D, Klein LC, Levy D, Schubert U, Wojcik AB (2003) In: Rappoport Z, Apeloig Y (eds) *The chemistry of organic silicon compounds*, vol 2. Wiley, Chichester
- Uchino T, Aboshi A, Kohara S, Ohishi Y, Sakashita M, Aoki K (2004) *Phys Rev B* 69:155409
- Corriu RJP, Gerbier P, Guerin C, Henner BJL, Jean AN, Mutin PH (1992) *Organometallics* 11:2507